ISSN: 2710-0588

Quantitative Assessment of Soybean Seedling Uniformity Based on Multi-Feature Fusion

Xueying Wen[1,*], Xiujuan Liang[1], Shiye Zhang[1] and Qingkai Liu[1]

[1] School of Surveying and Land Information Engineering, Henan Polytechnic University, Jiaozuo 454000, China

[*] Corresponding Author

Abstract

Accurate assessment of soybean seedling uniformity is essential for evaluating sowing quality and guiding early-stage field management, yet conventional manual inspection remains subjective and inefficient. This study presents a quantitative uniformity assessment framework based on multi-feature fusion using high-resolution RGB images. Per-plant masks and spatial positions are obtained through instance segmentation of soybean seedling images. Five categories of plot-level uniformity features are then extracted—emergence rate, plant spacing, inter-row angle, canopy coverage, and evenness index—along with their means, standard deviations, and coefficients of variation. An XGBoost classifier is trained to map these features to three uniformity grades, achieving an overall accuracy of 86.7% without cross-level misclassification. Feature importance analysis reveals that the standard deviation of plant spacing, emergence rate, and mean plant spacing emerge as the most influential predictors, providing explicit guidance for diagnosing the causes of poor uniformity. The proposed framework offers an interpretable and quantitative solution for automated seedling uniformity evaluation in soybean breeding programs.

Keywords

Soybean seedling uniformity; multi-feature fusion; XGBoost; feature importance; RGB imagery; precision agriculture.

1. Introduction

Crops seedling uniformity, reflecting the consistency of plant emergence and early growth across a field plot, is a critical agronomic trait for evaluating sowing quality and predicting subsequent canopy development. Uniform stands optimize the spatial utilization of light, water, and nutrients, reduce inter-plant competition, and form the foundation for high-yield canopy architecture [1,2]. Conversely, uneven emergence and irregular plant distribution often lead to growth suppression of weaker individuals, resulting in measurable yield losses [3]. In soybean breeding programs, rapid and objective uniformity assessment across large numbers of experimental plots is essential for variety screening and precision field management [4].

Despite its agronomic significance, seedling uniformity remains predominantly assessed through visual inspection by experienced breeders or agronomists in routine field trials . While such expert evaluation draws on valuable accumulated experience, it inherently suffers from subjectivity and variability among different evaluators, making it difficult to establish consistent and comparable standards across trials and locations [5]. Moreover, manual assessment becomes prohibitively time-consuming when hundreds or thousands of breeding plots must be evaluated within a narrow phenological window . The human eye, although capable of perceiving complex spatial patterns, cannot reliably quantify subtle differences in plant spacing variability, individual plant size distribution, or row alignment precision [6].

ISSN: 2710-0588

These limitations highlight the need for an automated, quantitative approach that can extract and integrate multiple objectively measurable indicators into a standardized uniformity score.

The rapid development of high-throughput phenotyping technologies has opened new possibilities for quantitative uniformity assessment [7]. Ground-based and unmanned aerial vehicle imaging platforms can now capture high-resolution RGB images covering large field areas within short time windows, preserving the spatial detail necessary for individual plant analysis . The key methodological challenge lies in translating these rich image data into meaningful uniformity metrics. Some approaches rely on vegetation indices or canopy cover statistics derived from multispectral or RGB imagery to describe spatial homogeneity at the canopy level . While efficient for large-scale screening, such methods operate on aggregate pixel information and cannot resolve individual plant-level variations in spacing, size, or morphology that collectively determine uniformity [8].

An alternative line of work has employed object detection or instance segmentation techniques to identify individual plants, from which plant-level traits can be extracted and statistically summarized [9]. This individual-to-population strategy aligns more closely with the agronomic definition of uniformity, which is fundamentally about the consistency among individual plants within a stand. For example, plant spacing variability, emergence rate, and the coefficient of variation of individual plant area have been proposed as quantitative surrogates for visual uniformity scores . However, existing studies have typically focused on a single or a narrow set of metrics, lacking a comprehensive framework that integrates multiple complementary dimensions of uniformity into a unified assessment. Furthermore, the relative importance of different contributing factors has rarely been quantitatively analyzed, limiting the diagnostic value of current methods for guiding specific management interventions[10] .

This study addresses these gaps by proposing a quantitative uniformity assessment framework that integrates multi-feature fusion with machine learning classification . Per-plant information is obtained through instance segmentation of high-resolution RGB images, from which five categories of plot-level features are computed: emergence rate, plant spacing, inter-row angle, canopy coverage, and evenness index. Each category includes the mean, standard deviation, and coefficient of variation, yielding a comprehensive set of statistical descriptors of within-plot uniformity. An XGBoost classifier is then trained to map these aggregated features to three uniformity grades defined by expert agronomist consensus. Beyond classification, feature importance analysis is conducted to identify the most influential predictors and to provide interpretable diagnostic insights into the specific causes of poor uniformity .

2. Materials and Methods

2.1. Data and Uniformity Grading

The soybean seedling images analyzed in this study were acquired from a field experiment conducted at the Dishang Experimental Station, Hebei Province, China, during the 2025 growing season. A fixed near-ground platform equipped with an industrial camera was used to capture high-resolution RGB images of soybean plots from a nadir view. Each image corresponded to a single plot planted with a distinct soybean variety. Per-plant masks and spatial coordinates were obtained through instance segmentation and served as the input for subsequent feature extraction.

To establish ground truth labels, three senior soybean breeders independently evaluated each plot image and assigned a uniformity score on a 1–10 scale, considering seedling size consistency, spatial distribution regularity, and the presence of missing plants or irregular rows. Plots were categorized into three uniformity grades based on the average of the three scores: L1 for scores of 1–3, representing poor uniformity; L2 for scores of 4–7, representing moderate uniformity; and L3 for scores of 8–10, representing good uniformity, The schematic diagram is

ISSN: 2710-0588

shown in Figure 1. When the standard deviation among evaluators exceeded 1.5, a consensus discussion was held to determine the final grade.

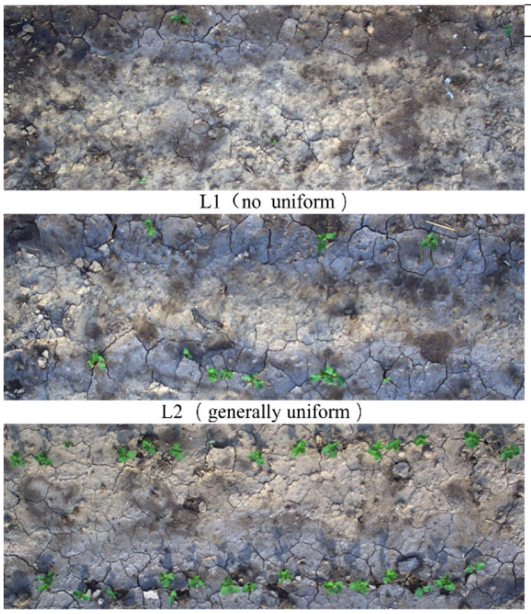

Level	Range of values	Key Feature Comparison
L1	1-3	There is a significant shortage of plants and they vary in size.
L2	4-7	Some plants are missing and the row alignment is incorrect.
L3	8-10	The plant spacing is relatively uniform and the sizes are relatively consistent.

Figure 1. Illustration of the classification of neatness levels and their main characteristics.

2.2. Uniformity Feature Extraction

Five categories of plot-level features were computed from the per-plant masks and spatial coordinates: emergence rate, plant spacing, inter-row angle, canopy coverage, and evenness index. For each category, three statistical descriptors were calculated: the mean, the standard deviation, and the coefficient of variation, yielding a total of 15 quantitative indices for every plot.

Emergence rate was defined as the ratio of the number of detected seedlings to the theoretical number of plants, calculated as

$$ER = \frac{N_{detected}}{N_{theory}} \times 100\% \quad (1)$$

where $N_{detected}$ is the number of seedlings identified through segmentation and N_{theory} is the expected number based on the known planting density and row length. This index captures the completeness of seedling establishment and identifies plots with missing plants.

Plant spacing was computed as the Euclidean distance between consecutive seedlings along the same row. Rows were identified by applying a Hough transform to the set of seedling center coordinates. After sorting seedlings by their projected positions along each detected row, the distance between successive plants i and i+1 was calculated as

$$Spacing = \sqrt{(x_{(i+1)} - x_i)^2 + (y_{(i+1)} - y_i)^2} \quad (2)$$

where (x_i, y_i) and (x_{i+1}, y_{i+1}) are the center coordinates of two adjacent seedlings in the same row. The mean spacing describes the average inter-plant distance within a plot, the standard deviation measures the variability of that distance, and the coefficient of variation expresses the variability relative to the mean.

ISSN: 2710-0588

Inter-row angle was measured as the acute angle between the two fitted row lines within each plot, expressed as

$$\text{Angle} = \min\left(\left|\alpha_1 - \alpha_2\right|, 180° - \left|\alpha_1 - \alpha_2\right|\right) \tag{3}$$

where α_1 and α_2 are the inclination angles of the two detected row lines. When rows are nearly parallel, the angle approaches zero; larger angles indicate deviations in row orientation likely caused by planting irregularities.

Canopy coverage was obtained by summing the pixel areas of all individual segmentation masks within a plot. The individual plant area was computed as

$$\text{Area} = \sum_{i=0}^{H-1}\sum_{j=0}^{W-1} P(i,j) \tag{4}$$

where $P(i,j)$ equals 1 for seedling pixels and 0 for background pixels within the segmentation mask of a given plant. The mean individual plant area reflects the average seedling size, the standard deviation captures size inequality among plants, and the coefficient of variation provides a scale-independent measure of size uniformity.

The calculation method of the uniformity index is as follows: divide the distance between each seedling and its nearest adjacent plant by the average plant spacing of the row. The result obtained is the index, denoted as EI. A value close to 1 indicates a regular spatial arrangement. Additionally, the ratio of the observed average plant spacing to the theoretical target plant spacing was calculated, denoted as ATEI, to quantify the deviation between the actual planting density and the designed density.

The mean, standard deviation, and coefficient of variation for all feature categories were calculated using the standard statistical formulas:

$$\overline{X} = \frac{1}{n}\sum_{i-1}^{n} X_i \tag{5}$$

$$\sigma_X = \sqrt{\frac{1}{n}\sum_{i-1}^{n}\left(X_i - \overline{X}\right)^2} \tag{6}$$

$$CV_X = \frac{\sigma_X}{\overline{X}} \times 100\% \tag{7}$$

where Xi represents the individual measurement for each seedling within a plot and n is the number of seedlings in that plot. Before model training, all features were standardized using Z-score normalization to remove the influence of differing measurement scales.

2.3. XGBoost Classification and Feature Importance Analysis

The XGBoost[11] algorithm was selected to construct the classification model mapping the 16 extracted features to the three uniformity grades. XGBoost is a gradient-boosted decision tree ensemble that has demonstrated strong performance on structured tabular data and offers built-in feature importance metrics, making it well-suited for both classification accuracy and interpretabilit. The model was built using the Python XGBoost library, which implements the scalable tree boosting system under a regularized objective function to prevent overfitting [12].

ISSN: 2710-0588

The dataset of 720 samples was randomly partitioned into training, validation, and test sets following an 8:1:1 stratified split, ensuring that the proportion of L1, L2, and L3 samples remained consistent across subsets. To address the class imbalance among the three grades, sample weights inversely proportional to class frequency were applied during training. The model was trained using the multi-class softmax objective with the following key hyperparameters optimized through grid search: a maximum tree depth of 6, a learning rate of 0.08, L1 regularization of 0.5, L2 regularization of 1.5, a subsample ratio of 0.8, and 800 boosting rounds. Early stopping was triggered when the validation loss failed to improve within 50 consecutive rounds. Hyperparameter tuning via grid search with cross-validation has been widely adopted in similar agricultural classification tasks [13].

Classification performance was evaluated using overall accuracy, precision, recall, and F1-score computed on the independent test set . A confusion matrix was generated to visualize the distribution of correct and incorrect classifications across the three uniformity grades.

The model evaluation system is constructed based on four basic statistics of the confusion matrix, namely: True Positive (TP): the number of samples correctly identified by the model as belonging to the corresponding category; False Positive (FP): the number of samples wrongly identified by the model as belonging to this category; False Negative (FN): the number of samples that are truly in this category but not correctly identified by the model; True Negative (TN): the number of samples correctly identified by the model as not belonging to this category. Overall Accuracy: The overall accuracy represents the proportion of samples that the model correctly classified out of the total number of samples, and is the most intuitive evaluation metric. The calculation formula is:

$$\text{Accuracy} = \frac{\text{TP} + \text{TN}}{\text{TP} + \text{TN} + \text{FP} + \text{FN}} \tag{8}$$

Beyond classification, the ability of XGBoost to quantify feature importance provides practical diagnostic value for this application. Feature importance scores were computed based on the average gain, which measures the improvement in accuracy brought by a feature when it is used as a split point across all trees in the ensemble [14]. This analysis identifies which specific aspects of uniformity are the most influential predictors of expert-assigned grades, enabling targeted interpretation of uniformity deficiencies in breeding practice.

3. Results

3.1. Feature Extraction and Distribution

The 16 uniformity features extracted from the 720 plot samples were analyzed across the three uniformity grades, and clear distributional differences were observed among L1, L2, and L3.

3.1.1. Emergence Rate

The emergence rate across all 720 plots exhibited an approximately normal distribution, with values concentrated primarily in the range of 0.5 to 0.8. The mean emergence rate was 0.656 and the median was 0.675, indicating that more than half of the plots achieved emergence rates exceeding 67.5% and that the overall seedling establishment was satisfactory. Plots with emergence rates below 0.5 accounted for a small proportion, as did those exceeding 0.8. This distribution is illustrated in Figure 2.

ISSN: 2710-0588

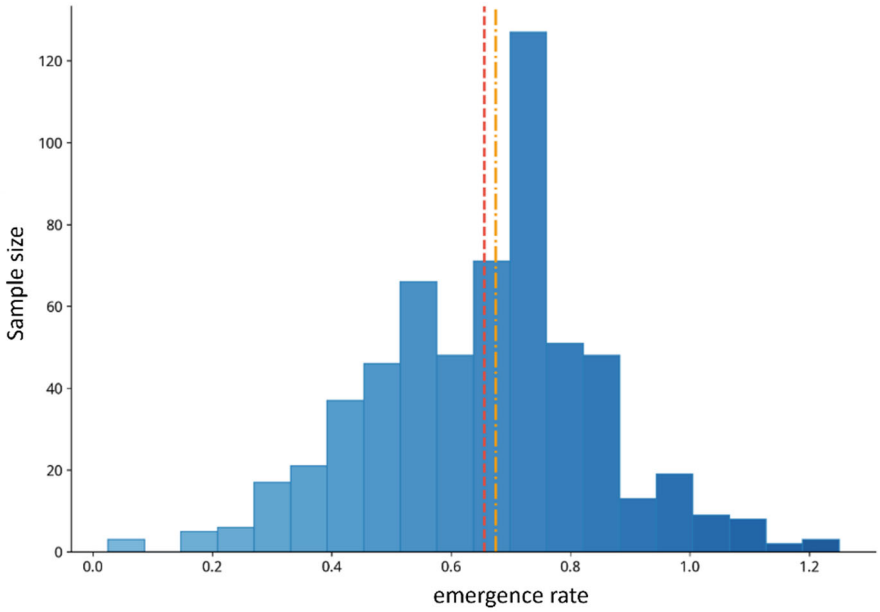

Figure 2. Distribution of emergence rate across all plots.

3.1.2. Emergence Rate

The remaining four categories of uniformity features are presented in Figure 3, including (a) spacing; (b) inter-row angle; (c) coverage; (d) uniformity index.

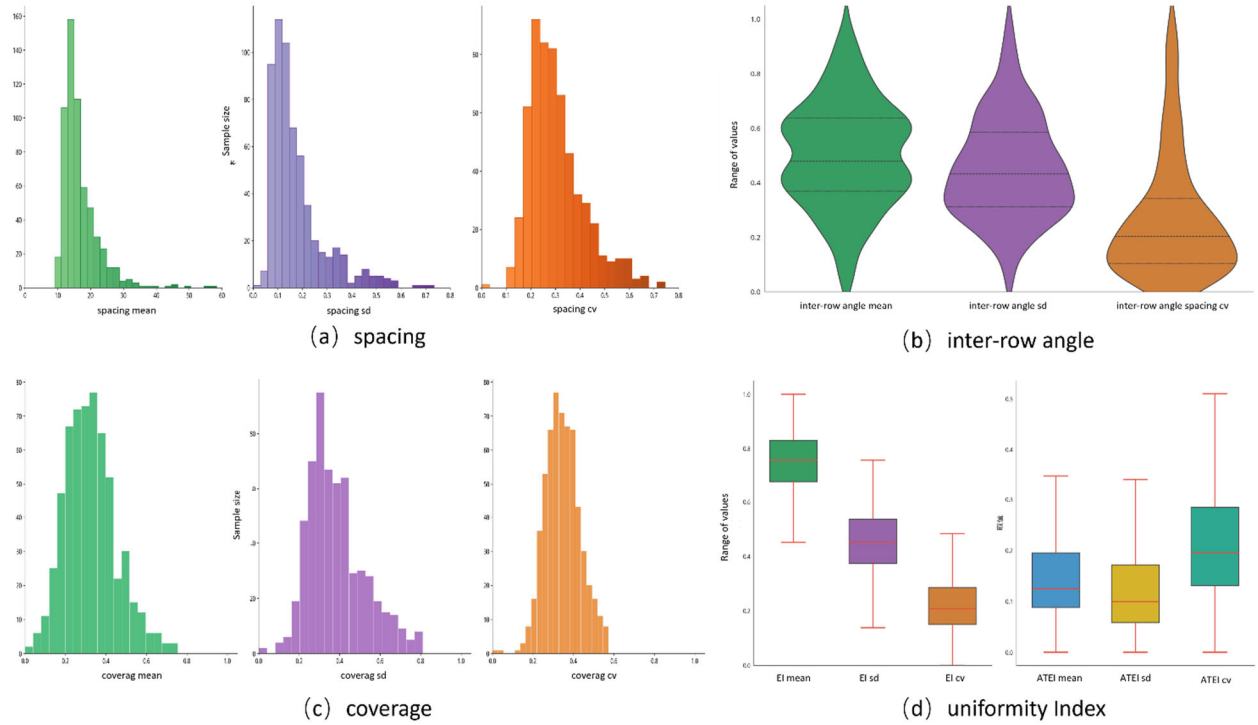

Figure 3. Distributions of uniformity features: (a) plant spacing; (b) inter-row angle; (c) canopy coverage; (d) evenness index.

The plant spacing indicators revealed specific patterns in sowing performance. The mean plant spacing across all plots was 16.88 cm, which exceeded the target spacing of 10 cm by a notable margin, indicating an overall wider spacing than designed. Despite this deviation, the distribution of mean spacing was compact, with most values concentrated within a narrow

ISSN: 2710-0588

interval, suggesting consistent planter operation across the experiment. The standard deviation of plant spacing was small, with a normalized mean of 0.175 and the majority of samples falling in the low range of 0 to 0.3, reflecting minimal within-plot spacing fluctuation. The coefficient of variation of plant spacing was the most concentrated of the three, with a normalized mean of 0.305, confirming high within-row planting precision and small between-plot differences in spacing regularity. The distributions of the three spacing indicators are shown in Figure 2(a).

The inter-row angle distribution was highly compact, with a normalized mean of 0.43 and a median of 0.43, and all values stably confined to the 0.4 to 0.6 range. Both the standard deviation and the coefficient of variation displayed similarly narrow distributions, demonstrating that the row orientation was highly consistent across the field and that the relative dispersion of row angles was low. The distributions of the three inter-row angle indicators are shown in Figure 2(b).

The canopy coverage feature, represented by the coefficient of variation of individual plant area, was concentrated mainly in the range of 0.25 to 0.45. This indicates that the majority of plots displayed limited within-plot plant size inequality, reflecting good seedling size uniformity across the field. The distributions of the three coverage indicators are shown in Figure 2(c).

The evenness index components exhibited stable and tightly clustered distributions. The coefficient of variation of EI was particularly low, while the coefficient of variation of ATEI had a mean of 0.22 and a median of 0.20. These values reflect very low relative dispersion and confirm that high spatial regularity was maintained across the experimental field. The distributions of the three evenness index indicators are shown in Figure 2(d).

3.2. Classification Performance

The XGBoost classifier was trained on the 16 extracted features to map each plot to one of the three uniformity grades. The confusion matrix on the independent test set is presented in Figure 4.

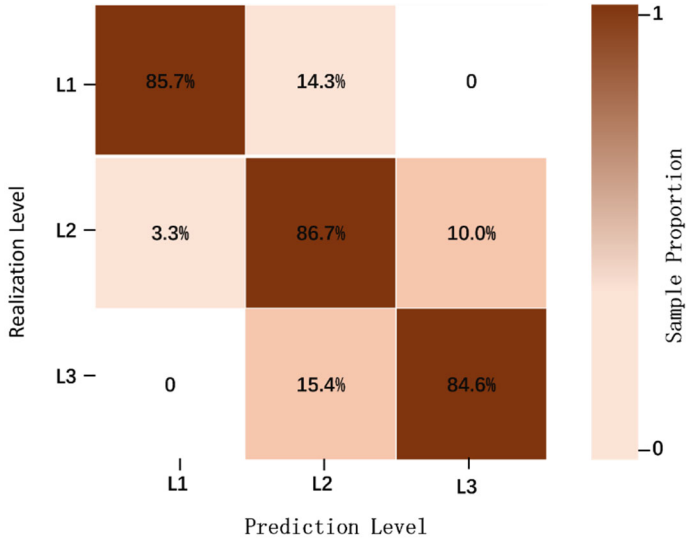

Figure 4. Confusion matrix of XGBoost classification on the test set.

As shown in Figure 4, the model achieved an overall classification accuracy of 86.7%. A key indicator of reliability is that no cross-level misclassification occurred: all classification errors were confined to adjacent grades. No plot labeled as L1 by the experts was misclassified as L3, nor was any L3 plot misclassified as L1. This indicates that while the boundary between adjacent grades remains somewhat difficult to resolve, the model possesses a robust overall judgment of seedling uniformity and does not confuse the extremes.

ISSN: 2710-0588

The per-class precision, recall, and F1-score are summarized in Table 1. The L1 grade achieved the highest precision at 90.0%, meaning that when the model predicted a plot as having poor uniformity, it was correct in the vast majority of cases. The recall for L1 was 85.7%, indicating that most truly poor-uniformity plots were successfully identified. The L2 grade, which had the largest number of samples, achieved a precision of 84.9% and a recall of 86.7%, demonstrating stable recognition of the majority class. The L3 grade achieved a precision and recall both at 84.6%. The macro-averaged F1-score was 0.86, and the weighted-averaged F1-score was also 0.86. The close agreement between these two averages confirms that the model performance was balanced across all three grades and was not biased toward the majority class.

Table 1. Classification performance by grade.

Level	Precision	Recall	F1-score
L1	0.90	0.86	0.88
L2	0.85	0.87	0.86
L3	0.85	0.85	0.85
macro avg	0.87	0.86	0.86
weighted avg	0.86	0.86	0.86
Accuracy		0.86	

The results demonstrate that the XGBoost classifier, when supplied with the 16 multi-dimensional uniformity features, can effectively replicate expert evaluations. The absence of cross-level errors is particularly important for practical breeding applications, where confusing a highly uniform plot with a highly non-uniform one could lead to incorrect selection decisions.

3.3. Feature Importance Analysis

To identify which specific aspects of uniformity contributed most to the classification decisions, feature importance scores were computed using the average gain metric from the trained XGBoost model. The top 10 features ranked by importance are presented in Figure 5.

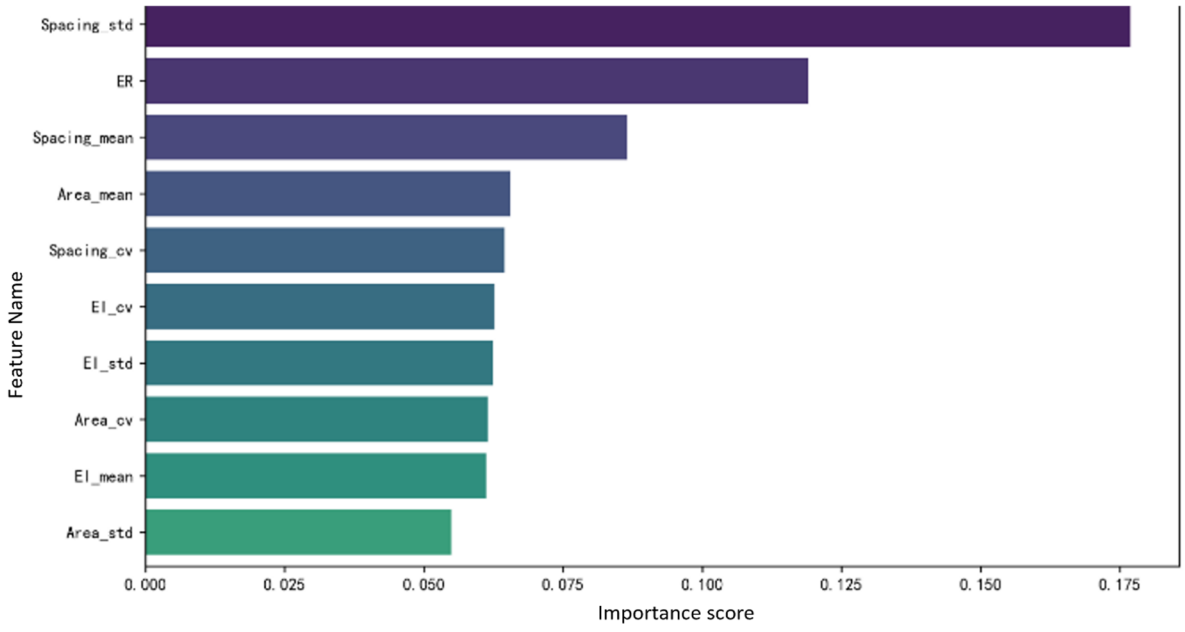

Figure 5. Feature Importance Analysis

ISSN: 2710-0588

The standard deviation of plant spacing emerged as the most influential predictor, with an importance score of 0.177, substantially higher than all other features. This result aligns closely with agronomic intuition: the variability of inter-plant distances within a row directly reflects planting uniformity, and larger spacing irregularities are the most visible indicator of poor stand establishment.

Emergence rate ranked second with an importance score of 0.12. As a direct measure of seedling establishment completeness, a low emergence rate indicates missing plants and gaps within the row, which are immediately apparent to expert evaluators. The combination of these two top features suggests that both the completeness of the stand and the regularity of plant distribution are the primary perceptual cues that experts rely on when judging uniformity.

Mean plant spacing ranked third with an importance score of 0.09, followed by the coefficient of variation of plant spacing. These spacing-related features collectively accounted for the largest share of total importance, confirming that within-row spatial patterns are the dominant determinant of uniformity grades.

Features related to individual plant size variability, including the standard deviation and coefficient of variation of plant area, together with the evenness index, each contributed importance scores ranging from 0.05 to 0.08. These features capture the consistency of seedling growth within a plot. Plots where individual plants differ substantially in size are perceived as less uniform even if the spacing is regular.

Features derived from the inter-row angle and the absolute mean plant area ranked relatively lower in importance. This suggests that expert evaluators placed greater weight on within-row spatial patterns and plant size consistency than on row alignment precision or the absolute magnitude of seedling size when forming their uniformity judgments.

The feature importance analysis not only validates the multidimensional feature design adopted in this study but also provides diagnostic value for breeding practice. When a plot is classified as having poor uniformity, the specific features contributing to that classification can be examined to identify the underlying cause, whether it is excessive spacing variability, low emergence, or uneven individual growth. This interpretability offers actionable guidance for field management interventions.

4. Conclusion

This study proposed a quantitative framework for assessing soybean seedling uniformity based on multi-feature fusion and machine learning classification using high-resolution RGB images. By extracting five categories of plot-level features—emergence rate, plant spacing, inter-row angle, canopy coverage, and evenness index—and aggregating their means, standard deviations, and coefficients of variation, a comprehensive set of 16 statistical descriptors was constructed to capture the multidimensional nature of seedling uniformity.

An XGBoost classifier trained on these features achieved an overall accuracy of 86.7% in classifying plots into three uniformity grades, with no cross-level misclassification between the extremes. The macro-averaged and weighted-averaged F1-scores both reached 0.86, confirming balanced performance across grades despite class imbalance. Feature importance analysis revealed that the standard deviation of plant spacing was the single most influential predictor, followed by emergence rate and mean plant spacing, collectively accounting for nearly 40% of the total importance. This finding provides quantitative evidence that within-row spacing variability and stand completeness are the primary perceptual cues underlying expert uniformity evaluation.

The proposed framework offers two distinct advantages for breeding practice. It replaces subjective visual inspection with objective, repeatable quantitative metrics, thereby enabling standardized uniformity assessment across trials and locations. Furthermore, the

ISSN: 2710-0588

interpretability afforded by feature importance analysis allows breeders to diagnose the specific causes of poor uniformity—whether excessive spacing variability, low emergence, or uneven individual growth—and to implement targeted management interventions. Future work will focus on extending this framework to UAV-based imagery for large-scale field phenotyping and on integrating the assessment pipeline into automated breeding decision support systems.

5. Discussion

The proposed framework offers an objective alternative to subjective visual scoring, which remains the standard practice in soybean breeding trials. By decomposing uniformity into five measurable feature categories and aggregating their statistical descriptors, the framework captures the multidimensional nature of stand quality in a way that is both comprehensive and interpretable. The alignment between feature importance rankings and agronomic intuition, where spacing variability and emergence completeness dominate, confirms that the selected features meaningfully encode the perceptual cues used by expert evaluators. The ability to isolate specific causes of poor uniformity through feature importance analysis distinguishes this approach from both traditional visual scoring and end-to-end image classification methods.

Compared with canopy-level assessment methods based on aggregate vegetation indices, the individual-to-population approach adopted here offers finer diagnostic resolution. Canopy-level methods can flag plots with gross spatial heterogeneity but cannot distinguish, for example, between a plot with missing plants and one with highly uneven individual growth. The feature-driven classification framework provides this distinction without sacrificing interpretability, making it possible to trace a uniformity grade back to its constituent factors.

Several limitations should be acknowledged. The dataset was collected from a single experimental station during one growing season, and the observed feature distributions may not generalize to other environments or genotypes. Future work should validate the framework across multiple sites and seasons and explore its extension to UAV-based imagery for large-scale field phenotyping.

Acknowledgements

The authors gratefully acknowledge the Institute of Cereal and Oil Crops, Hebei Academy of Agriculture and Forestry Sciences, for providing the experimental site and field management support. The authors also thank the experts who participated in the uniformity grading of soybean seedling images.

References

[1] Siega G A, Filho A C P de M, Sharma P, et al. Influence of planting speed on emergency uniformity and distribution of soybean plants[J]. Cerrado: Agricultural and Biological Research, 2024, 1(2): 21-29.

[2] Shirzadifar A, Maharlooei M, Bajwa S G, et al. Mapping crop stand count and planting uniformity using high resolution imagery in a maize crop[J]. Biosystems Engineering, 2020, 200: 377-390.

[3] Hue Y, Kim J H, Nam Y, et al. Changes in the occurrence patterns of rice fungal diseases due to climate change[J]. Research in Plant Disease, 2025, 31(1): 17-29.

[4] Zhou J, Beche E, Vieira C C, et al. Improve soybean variety selection accuracy using UAV-based high-throughput phenotyping technology[J]. Frontiers in Plant Science, 2022, 12.

[5] Zarei E, Yazdi M, Moradi R, et al. Expert judgment and uncertainty in sociotechnical systems analysis[M]//ZAREI E. Safety causation analysis in sociotechnical systems: advanced models and techniques. Cham: Springer Nature Switzerland, 2024: 487-530.

ISSN: 2710-0588

[6] Zhou J, Cui M, Wu Y, et al. Maize (zea mays L.) stem target region extraction and stem diameter measurement based on an internal gradient algorithm in field conditions[J]. Agronomy, 2023, 13(5): 1185.

[7] Yuan H, Song M, Liu Y, et al. Field phenotyping monitoring systems for high-throughput: a survey of enabling technologies, equipment, and research challenges[J]. Agronomy, 2023, 13(11): 2832.

[8] Zhang Q, Luan R, Wang M, et al. Research progress of spectral imaging techniques in plant phenotype studies[J]. Plants, 2024, 13(21): 3088.

[9] Weyler J, Magistri F, Seitz P, et al. In-field phenotyping based on crop leaf and plant instance segmentation[C]//Proceedings of the IEEE/CVF Winter Conference on Applications of Computer Vision. 2022: 2725-2734.

[10] Vargo M, Aldrich M, Donahue P, et al. Current diagnostic and quantitative techniques in the field of lymphedema management: a critical review[J]. Medical Oncology, 2024, 41(10): 241.

[11] Chen T, Guestrin C. XGBoost: a scalable tree boosting system[C]//Proceedings of the 22nd ACM SIGKDD International Conference on Knowledge Discovery and Data Mining. New York, NY, USA: Association for Computing Machinery, 2016: 785-794.

[12] Demir S, Sahin E K. An investigation of feature selection methods for soil liquefaction prediction based on tree-based ensemble algorithms using AdaBoost, gradient boosting, and XGBoost[J]. Neural Computing and Applications, 2023, 35(4): 3173-3190.

[13] Al Kaddouri H, Blaacha J, Hamdaoui H, et al. Optimization of hyperparameters for SVM classification of citrus diseases using grid search and cross-validation[C]//Proceedings of the 4th International Conference on Electronic Engineering and Renewable Energy Systems—Volume 1. Springer, Singapore, 2025: 489-497.

[14] Alhams A, Abdelhadi A, Badri Y, et al. Enhanced bearing fault diagnosis through trees ensemble method and feature importance analysis[J]. Journal of Vibration Engineering & Technologies, 2024, 12(1): 109-125.